Gravitational model of high energy particles in a collimated jet

J.A. de Freitas Pacheco[1]

[1]University of Nice-Sophia Antipolis, Observatoire de la Côte d'Azur

Laboratoire Lagrange, UMR 7293, BP 4229, 06304 Nice Cedex 4, France

pacheco@oca.eu

J. Gariel[2] and G. Marcilhacy[2]

[2]LERMA - UPMC, University Pierre and Marie Curie, Observatoire de Paris

CNRS, UMR 8112, 3 rue de Galilée, 94200 Ivry sur Seine, France

jerome.gariel@upmc.fr,gmarcilhacy@hotmail.com

and

N.O. Santos[2,3]

[3]School of Mathematical Sciences, Queen Mary, University of London

Mile End Road, London E1 4NS, United Kingdom

nilton.santos@upmc.fr

ABSTRACT

Observations suggest that relativistic particles play a fundamental role in the dynamics of jets emerging from active galactic nuclei as well as in their interaction with the intracluster medium. However, no general consensus exists concerning the acceleration mechanism of those high energy particles. A gravitational acceleration mechanism is here proposed, in which particles leaving precise regions within the ergosphere of a rotating supermassive black hole produce a highly collimated flow. These particles follow unbound geodesics which are asymptotically parallel to the spin axis of the black hole and are characterized by the energy E, the Carter constant $\mathcal{Q}$ and zero angular momentum of the component L_z. If environmental effects are neglected, the present model predicts at distances of about 140 kpc from the ergosphere the presence of electrons with energies around 9.4 GeV. The present mechanism can also accelerate protons up to the highest energies observed in cosmic rays by the present experiments.

Subject headings: Kerr geodesics, astrophysical jets, high energy particles

1.   Introduction

Multiwavelength observations of different astrophysical objects indicate the presence of "jets" (Marscher 2005) driven probably by a compact object like a black hole (BH) or, in some cases, a highly magnetized rotating neutron star. Jets are observed at scales ranging from sub-parsec up to hundreds of kiloparsec. Gamma-ray bursts are an example of small scale jets, since they are supposed to be the consequence of shocks occurring in highly collimated relativistic flows (Mészáros et al. 1999; Frail et al. 2001; Rossi et al. 2002) originated either at the death of a massive star or when a neutron star merges with another neutron star or with a black hole. Large scale jets are observed in association with radio-galaxies, quasars, blazars or AGNs (active galactic nuclei) in general and their origin is probably the consequence of the twisting of magnetic fields anchored in the very inner region of an accreting disk around a supermassive black hole (Blandford & Levinson 1995; Meier et al. 2000; Camenzind 2005).

Jets associated with AGNs have a complex structure with bulk motions characterized by Lorentz factors typically in the range 10-50 and total power ranging from 10^{44} up to 10^{47} ergs^{-1}. The composition of these flows is still uncertain but, in general, supposed to be constituted by electrons and protons or/and electron-positron pairs or even heavy nuclei. The composition of the jet is certainly related to the physical processes that create and energize the flow, representing an important key for the understanding of the launching mechanism. The large scale acceleration required to explain the high velocities of the bulk motion cannot be purely hydrodynamic and are probably a manifestation of the presence of extended magnetic pressure gradients (Vlahakis & Konigl 2004). Fully relativistic simulations of accretion disks around a rotating black hole indicate that unbound flows can emerge self-consistently from the accretion flow (De Villiers et al. 2005). According to these simulations, the flow has two main components: a hot, fast and tenuous outflow

along the jet axis and a cold, slow and dense flow along the funnel wall defining the jet geometry (see also Meliani & Keppens 2009). For slow rotating BHs, the flow energetics is dominated by the kinetic energy and the enthalpy of matter whereas for fast rotating BH the energetics is essentially given by a Poynting flux. Jets dominated by kinetic energy penetrate easily in the intra-cluster medium (ICM), forming low density cavities elongated in the radial direction (Guo & Mathews 2011). This is not the case if the energetics of the jet is dominated by highly relativistic particles. In this case, due to the low inertia, the jet decelerates rapidly in the ICM, producing large cavities due to the lateral expansion produced by the pressure of the relativistic particles (Guo & Mathews 2011).

The result of these simulations emphasize the importance of the presence of relativistic particles in the jet, either to characterize the dynamics of the flow or the interaction with the ICM. However, the acceleration mechanism (or mechanisms) of these relativistic particles is not yet well understood although magnetohydrodynamic shocks and Fermi-like mechanisms are often invoked as possibilities. Here we examine a completely different alternative, i.e., a purely gravitational acceleration process based on the presence of an ergosphere around a Kerr BH. In our scenario, we assume that an accreting rotating BH is present in the center of an active galaxy. Matter penetrating the ergosphere can undergo the Penrose process (Penrose 1969) and, under certain conditions, the emerging particles follow geodesics asymptotically parallel to the rotation axis, acquiring very high energies. Although the efficiency of the Penrose process is still a matter of debate, this important question will be not examined in the present paper.

The existence of unbound geodesics leaving the ergosphere along the z-axis and focusing at infinity was already demonstrated by Gariel et al. (2010, hereafter GMMS10). In the present work, it is shown that test particles, independently of their electric charge, following these highly collimated geodesics, model a narrow energetic beam in precise regions of the

ergosphere. The present investigation is addressed to the study of some particular solutions describing those geodesics as well as to the analysis of the initial conditions required for their existence. The paper is organized as follows: in Section 2, the constants of motion, the total particle energy E and the Carter constant $\mathcal{Q}$ are derived as functions of two real roots of the characteristic equation $R^2(r) = 0$, where the function R governs the timelike geodesics in the Kerr's metric; Section 3 is dedicated to the study of the particular case in which a double root of the equation $R^2(r) = 0$ exists. It is shown that high particle energy values are possible only for two narrow ranges of values of the considered double root; in Section 4 the two remaining roots of the characteristic equation are examined as well as the consequences for the allowed values of E and for the asymptotes of the geodetic motion; in Section 5 an analysis of these various solutions is performed, permitting to restrict to one the different possibilities and, finally, in Section 6 the main conclusions are given.

2.   The constants of motion

Firstly, it should be emphasized that our model is highly idealized since interactions with the ambient medium or with magnetic fields, which affect the motion and the energy budget of particles, are not included in the present approach and will be considered in a future paper. This investigation will be focused on the study of the motion of test particles following unbound geodesics along the z-axis, under the assumption that the central supermassive black hole (SMBH) rotates steadily.

Assuming an axisymmetric geometry, the generalized cylindrical or Weyl coordinates (ρ, z, ϕ), related to Boyer-Lindquist generalized spherical coordinates (r, θ, ϕ) by

$$\rho = [(r-1)^2 - A]^{1/2} \sin\theta, \;\; z = (r-1)\cos\theta \tag{1}$$

where

$$A = 1 - \left(\frac{a}{M}\right)^2 \tag{2}$$

are the most suitable for describing the system. As already mentioned, the existence of special unbound geodesics in this frame was recently demonstrated by GMMS10. These geodesics stem from the ergosphere and when $z \to \infty$, they are asymptotically parallel to the z axis and positioned at distance

$$\rho = \rho_1 \equiv \left(\rho_e^2 + \frac{\mathcal{Q}}{E^2 - 1}\right)^{1/2} \tag{3}$$

that depends on $\rho_e \equiv a/M$ and on two constants of motion; the Carter constant $\mathcal{Q}$ and the energy E, while the third constant of motion, the z component of the angular momentum L_z is necessarily null.

The function $R(r)$ (see, for instance, Chandrasekhar 1983) introduced in the expression of the Kerr timelike geodesics (test particle mass $\sqrt{\delta_1} = 1$) plays a fundamental role in the analysis of the jet collimation when the engine at the centre of the accretion disk is supposed to be a stationary rotating SMBH. This function is a fourth order polynomial, i.e.,

$$R^2(r) = a_4 r^4 + a_3 r^3 + a_2 r^2 + a_1 r + a_0 \tag{4}$$

where the coefficients, excepting a_3, depend on the constants of motion and on the BH parameters (Chandrasekhar 1983) as

$$a_0 = -a^2 \mathcal{Q}, \ \ a_1 = 2(a^2 E^2 + \mathcal{Q})$$
$$a_2 = a^2(E^2 - 1) - \mathcal{Q}, \ \ a_3 = 2, \ \ a_4 = E^2 - 1 \tag{5}$$

Without loss of generality, we have put $M = 1$ and $L_z = 0$ when considering the special 2D-geodesics given by Equation (3). Hence, the spin a of the SMBH being fixed $(-1 \leq a \leq 1)$, we have two independent parameters left, $\mathcal{Q}$ and E, or, equivalently from Equation (3), the position ρ_1 of the asymptote parallel to the z-axis and the energy E.

Let us consider the possible roots of the equation $R^2(r) = 0$ of the characteristics $\dot{r} = 0$ of the autonomous system of geodesics equations (Chandrasekhar 1983), i.e.,

$$a_4 r^4 + a_3 r^3 + a_2 r^2 + a_1 r + a_0 = 0 \tag{6}$$

The polynomial given by Equation (6) has four roots, labeled r_i with $i = 1, 2, 3, 4$, which can be *a priori* real (positive or negative) or complex (contrary to the physical variable r, which is always real and defined in the interval $\left[1 + \sqrt{A}, \infty\right)$. The two equations $R^2(r_1) = 0$ and $R^2(r_2) = 0$ are linear in $\mathcal{Q}$ and $(E^2 - 1)$. Thus, the solution of this linear system permits to express the constants of motion as functions of the roots r_1 and r_2, namely

$$\mathcal{Q} = \frac{2 r_1 r_2}{D} \left\{ a^4 + a^2 \left[r_1(r_1 - 2) + r_2(r_2 - 2) \right] + r_1^2 r_2^2 \right\} \tag{7}$$

and

$$(E^2 - 1) = -\frac{2}{D} \left\{ a^4 + a^2 (r_1^2 + r_2^2) + r_1 r_2 \left[r_1(r_2 - 2) - 2 r_2 \right] \right\} \tag{8}$$

with the denominator D given by

$$D = a^4 (2 + r_1 + r_2) + a^2 \left[r_1^3 + r_1^2 r_2 + r_1 r_2 (r_2 - 4) + r_2^3 \right] + r_1 r_2 \left[(r_1^2 + r_1 r_2)(r_2 - 2) - 2 r_2^2 \right]. \tag{9}$$

In the third possible equation, $R^2(r_3) = 0$, the parameters $\mathcal{Q}$ and $E^2 - 1$ can be replaced by Equations (7) and (8), leading to a relation between r_3, r_1 and r_2, allowing in principle, to determine the values of r_3 as a function of r_1 and r_2 only, since the spin parameter a is fixed. The fourth possible equation, $R^2(r_4) = 0$, does not represent any new result since the roots r_3 and r_4 are the same.

In Equations (7) and (8), it is worth noting the symmetric role of r_1 and r_2, and that $\mathcal{Q}$ and $E^2 - 1$ have the same denominator D. Thus, if and only if, it cancels, we have both $E \to \infty$ and $|\mathcal{Q}| \to \infty$, whereas ρ_1, since it depends only on their ratio (see Equation (3)), tends towards a finite value. From Equations (3), (7) and (8) we obtain for the position of

the asymptotes

$$\left(\frac{\rho_1}{\rho_e}\right)^2 = \frac{(a^2 + r_1^2)(a^2 - r_1 r_2)(a^2 + r_2^2)}{a^2 \left\{a^4 + a^2(r_1^2 + r_2^2) + r_1 r_2 \left[r_1(r_2 - 2) - 2r_2\right]\right\}} \tag{10}$$

It should be emphasized that the roots r_1 and r_2, satisfying the condition $D = 0$, for a given value of the spin parameter a, permit to define regions in the ergosphere from which unbound geodesics parallel to the z-axis emerge, along which move particles with "quasi"-infinite energies and that could eventually explain the very energetic particles observed in cosmic rays. We will return to this point later.

3.   Real roots $r_1 = r_2$

In order to simplify the mathematical analysis and without loss in the physical insight, we assume in this paper the particular case in which a double real root $r_1 = r_2 = Y$ exists. Under this assumption Equation (4) can be recast as

$$R^2(r) = a_4(r - Y)^2(r^2 + Br + C) \tag{11}$$

and Equations (7) and (8) simplify as

$$\mathcal{Q} = \frac{[a^4 + 2a^2(Y - 2)Y + Y^4]Y^2}{a^4(1 + Y) + 2a^2(Y - 1)Y^2 + (Y - 3)Y^4} \tag{12}$$

and

$$E^2 - 1 = -\frac{a^4 + 2a^2Y^2 + (Y - 4)Y^3}{a^4(1 + Y) + 2a^2(Y - 1)Y^2 + (Y - 3)Y^4} \tag{13}$$

When $E \to \infty$, of course we have also $|\mathcal{Q}| \to \infty$ but, as already mentioned, their ratio tends towards a finite value in order that the coordinate ρ_1 remains finite, i.e.,

$$\left(\frac{\rho_1}{\rho_e}\right)^2 = \frac{(a^2 - Y^2)(a^2 + Y^2)^2}{a^2[a^4 + 2a^2Y^2 + (Y - 4)Y^3]} \tag{14}$$

In order to perform some numerical estimates, we will assume, unless otherwise stated, a "moderate" rotation for the SMBH, fixing $a = M/2$ (a value adopted already by GMMS10

in their investigation). Hence, the functions $E^2 - 1 \equiv F(Y)$ and $(\rho_1/\rho_e)^2 \equiv G(Y)$ can be plotted as shown in Figures 1 and 2.

Since $F(Y)$ and $G(Y)$ must be simultaneously positive, the only possible solutions correspond to the two intervals

$$Y \in [-0.5, Y_{0a}] \tag{15}$$

and

$$Y \in [Y_{0b}, 3.8697] \tag{16}$$

with Y_{0a} and Y_{0b} being asymptotes of $F(Y)$ for which $E \to \infty$. These asymptotes can be evaluated numerically since they correspond to the roots of the equation $D = 0$. For the assumed BH parameters, it results $Y_{0a} \simeq -0.2418$ and $Y_{0b} \simeq 2.8832$.

Hence, there are only two possible values of ρ_1 for which $E \to \infty$, corresponding to the two intervals defined above. For these limits, $Y = Y_{0a} - \varepsilon$ and $Y = Y_{0b} + \varepsilon$, when $\varepsilon \to 0$, we obtain respectively for the coordinate ρ_1

$$\frac{\rho_1}{\rho_e} \simeq 0.6932 \quad \text{and} \quad \frac{\rho_1}{\rho_e} \simeq 10.2411. \tag{17}$$

For the upper bound of the interval (16), i.e., for $Y = 3.8697$ where $\rho_1 \to \infty$, we have $E^2 - 1 = 0$ and, for the lower bound of the interval (15), i.e., for $Y = -0.5$ where $E^2 - 1 = 2$, we have $\rho_1 = 0$.

When $r_1 \neq r_2$, the problem is quite difficult and a more careful study is necessary. This is presently underway and will be reported in a future paper. Nevertheless, the following aspects may be anticipated. As we have seen, in the case of a double root, geodesics followed by particles of sufficient high energy ($E > 3$), remain clustered around values of ρ_1 corresponding to $E \to \infty$. Moreover, in the general case the condition $D(r_1, r_2) = 0$ defines the regions from which high energy geodesics emerge. The later condition is given by a third order polynomial in r_2, which has a unique real root that can be explicited as a function of
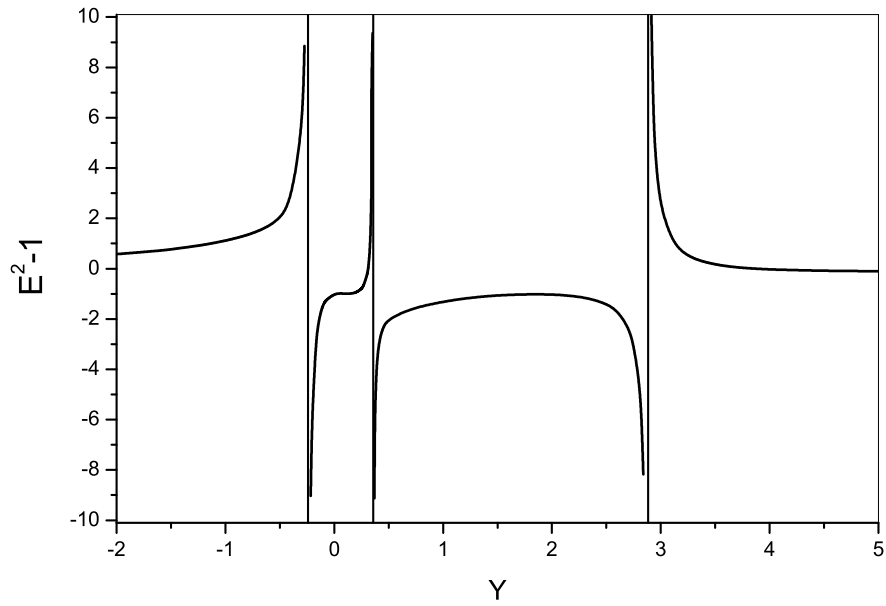
Fig. 1.— Plot of $E^2 - 1 \equiv F(Y)$, where E is the energy of the test-particle as a function of the double root Y, computed from Equation (13) for a BH of mass $M = 1$ and spin parameter $a/M = 0.5$. The values of Y for which $E^2 - 1$ is positive, as expected for unbound geodesics, are clearly seen as well as the three values of Y for which $E^2 - 1$ tends (positively) to infinity.
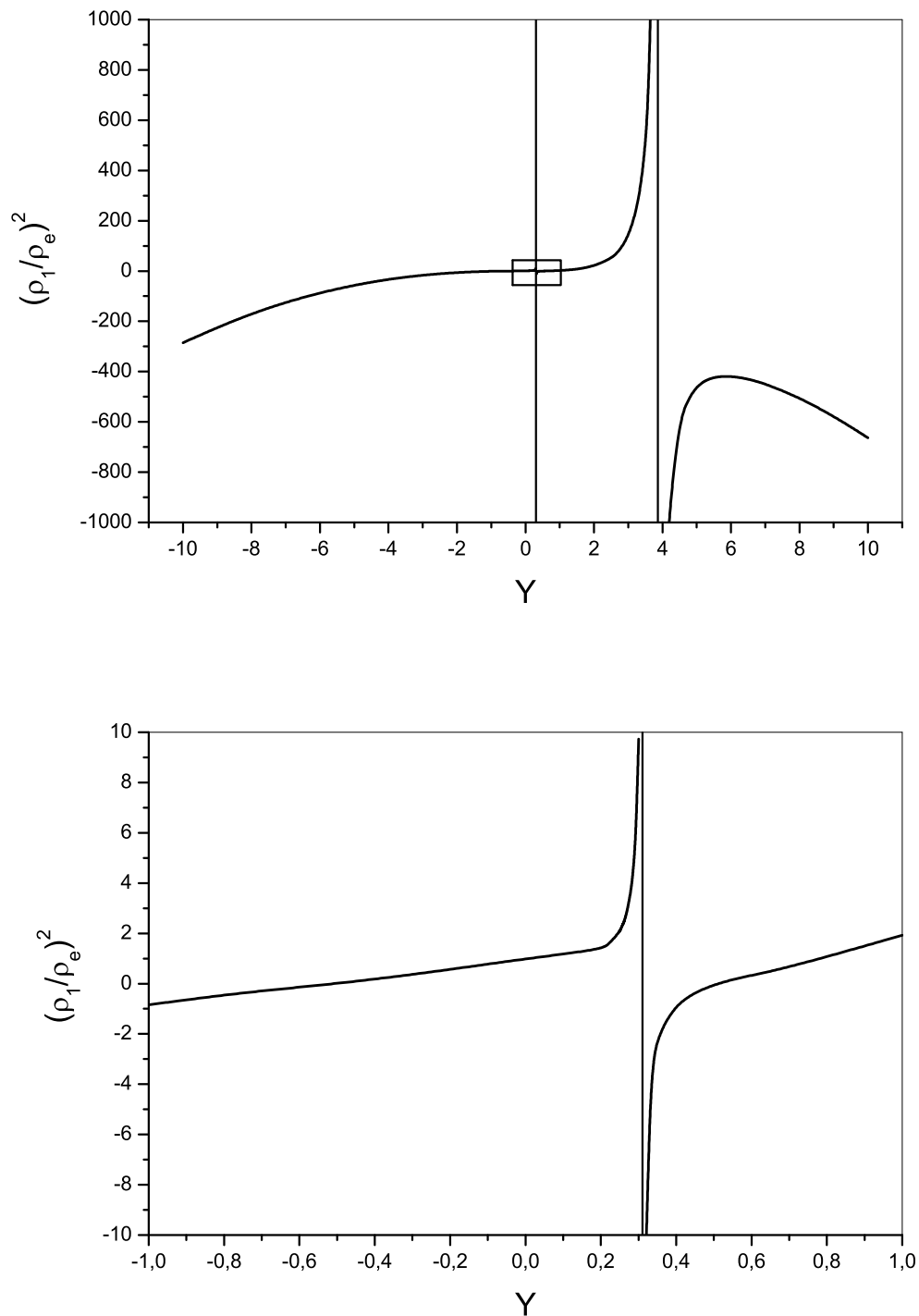
Fig. 2.— **Upper panel**: Plot of the ratio $(\rho_1/\rho_e)^2$ as function of the double root Y, evaluated from Equation (14), for a BH of mass $M = 1$ and spin parameter $a/M = 0.5$. The intervals of Y in which the ratio $G(Y)$ is positive can be seen. **Lower panel**: details of the variation of the ratio $G(Y)$ corresponding to the rectangle shown in the upper panel.

r_1. This can be inserted into Equation (10) defining the position of the asymptote ρ_1 as a function only of r_1. That leads again to very restricted ranges of possible values of ρ_1.

For the sake of completeness and in order to investigate also the possible influence of the spin parameter in our analysis, we have also considered the case of a extreme Kerr black hole ($a/M = 1$). The results are qualitatively the same. The only physical solution leading to $E \to \infty$ corresponds to the double root Y=-0.4142 and to an asymptote whose position is $\rho_1 \simeq 0.8284$.

4. Roots r_3 and r_4

Identifying Equation (11) with Equation (4), rewritten in terms of the parameters $E^2 - 1 = F(Y)$ and $(\rho_1/\rho_e)^2 = G(Y)$, without the explicit form of these functions of Y (see Equations (13) and (14)), yield the four relations,

$$B - 2Y = \frac{2}{F}, \;\; G + \frac{1}{F} = 2Y(BY - 2C),$$
$$1 - G = 16CY^2, \;\; 2 - G = 4(C - 2YB + Y^2), \tag{18}$$

which are linear in $1/F$, G, B and C. After eliminating $1/F$ and G, we obtain from the equations above

$$B = -\frac{2(4Y^2 - 1)[Y(4Y - 1) + Y - 1]}{(4Y^2 - 1)^2 - 16Y^2(4Y - 1)}, \tag{19}$$

$$C = \frac{(4Y^2 - 1)^2 + 16Y(Y - 1)}{4[(4Y^2 - 1)^2 - 16Y^2(4Y - 1)]}. \tag{20}$$

Hence Equation (11) can be recast as

$$R^2 = a_4(r - Y)^2(r^2 - Sr + P) \tag{21}$$
$$= a_4(r - Y)^2(r - r_3)(r - r_4),$$

where r_3 and r_4 are the remaining roots, in general distinct, and we have introduced

$$S \equiv r_3 + r_4 = -B, \;\; P \equiv r_3 r_4 = C, \tag{22}$$

or

$$r_3 = -\frac{1}{2}\left[B + \left(B^2 - 4C\right)^{1/2}\right], \tag{23}$$

$$r_4 = -\frac{1}{2}\left[B - \left(B^2 - 4C\right)^{1/2}\right], \tag{24}$$

where $B(Y)$ and $C(Y)$ are given respectively by Equations (19) and (20).

The curves $r_3(Y)$ and $r_4(Y)$ are real only for some well defined ranges of Y. In particular, in the interval (15) defining Y, r_3 and r_4 are not real. In order to have the expression $r^2 + Br + C$ in Equation (11) real, where B and C are real, r_3 and r_4 have to be complex conjugated, i.e., $r_3 = z = B_1 + iC_1$ and $r_4 = \bar{z}$. Hence, the sign of the expression $r^2 + Br + C = (r + B_1)^2 + C_1^2$ is always positive, and $P = C = B_1^2 + C_1^2 \geq 0$ and $S = -B = -2B_1 \leq 0$.

In the interval (16), the two roots r_3 and r_4 are real, $P = C$ is negative (which means two roots of opposite signs) and $B = -T$ is positive. The most precise value we have numerically obtained for the left limit (where, in principle, $E \to \infty$) of the range (16) allows us to reach the value $E \simeq 1.1 \times 10^{32}$. Then, the corresponding real values of the roots are respectively $r_3 = -5.8988$ and $r_4 = 0.1324$.

Also, it is worth observing that E is steeply decreasing either for a weak variation ε of Y from Y_{0b} ($\varepsilon > 0$) or from Y_{0a} ($\varepsilon < 0$), while ρ_1 is weakly increasing for this same small interval of Y. For example, when Y goes from Y_{0b} to 2.922, the energy E is steeply decreasing from 10^{30} to 3, while the position of the asymptote ρ_1/ρ_e increases by a small amount from 10.24 to 10.68, which means a large concentration of the most energetic part (the "spine") of the beam immediately near at the right hand side of $\rho_1/\rho_e = 10.24$. At its left hand side, there is no beam produced.

Likewise, for the interval (15), the energy E is very steeply decreasing from "infinity" to 6. Within our numerical precision, when $Y \to Y_{0a}$, the highest value obtained for the

energy was $E_{max} \simeq 2 \times 10^{30}$. The corresponding asymptote ρ_1/ρ_e inside the ergosphere decreases very slightly from 0.6932 to 0.6764. Here the jet is still more concentrated just at the left of coordinate value 0.6932, while beyond its right side, there is no beam at all.

As a result, the present model predicts a radial structure of the "jet", with a well defined profile for the energy (or velocity) distribution of the particles.

5.   Unbound geodesics for high energy particles

Now let us consider the set of possible energetic geodesics framing a jet and their corresponding asymptotes, satisfying the conditions considered in the previous section. In this case, the choice of admissible initial conditions (IC) depends strongly on their positions relative to the characteristics of the system of geodesic equations (see Equations (2) and (3) in GMMS10). Indeed, each characteristic separates the plane into two regions and a given geodesic cannot cross the borders defined by those curves. In Boyer-Lindquist coordinates, the characteristics are defined by the equations

$$\dot{r} = 0, \quad \dot{\theta} = 0, \tag{25}$$

each of which is equivalent to the equations,

$$R(r) = 0, \quad T(\theta) = 0, \tag{26}$$

respectively, where $R(r)$ is given by Equation (4) and $T(\theta)$ by

$$T(\theta) = -(b_4\mu^4 + b_2\mu^2 + b_0)^{1/2}, \tag{27}$$

with $\mu = \cos\theta$ and

$$b_0 = \frac{\mathcal{Q}}{M^2}, \quad b_2 = a_2, \quad b_4 = -\left(\frac{a}{M}\right)^2 (E^2 - 1). \tag{28}$$

The solutions of Equation (26), when they exist, are the roots r_i and the roots θ_i, which define respectively circles and straight lines from the origin.

In Weyl coordinates ρ and z, each characteristic Equation (25) is equivalent to the equations (see Equations (17) and (18) in GMMS10)

$$\dot\rho = \frac{R(\alpha^2 - A)z}{\alpha\rho\Delta}, \quad \dot z = -\frac{R\alpha}{\Delta}, \tag{29}$$

and

$$\dot\rho = \frac{T\alpha^3\rho}{(\alpha^2 - A)\Delta}, \quad \dot z = \frac{T\alpha z}{\Delta}, \tag{30}$$

respectively, where

$$\Delta = (\alpha + 1)^2\alpha^2 + \left(\frac{a}{M}\right)^2 z^2. \tag{31}$$

Each set of Equations (29) and (30) leads to

$$\frac{dz}{d\rho} = -\frac{\alpha^2\rho}{(\alpha^2 - A)z}, \tag{32}$$

and

$$\frac{dz}{d\rho} = \frac{(\alpha^2 - A)z}{\alpha^2\rho}, \tag{33}$$

respectively, defining the two families of characteristics for the geodesics of type Equation (25) in which we are interested, namely, ellipses (corresponding to $\dot r = 0$) and hyperbolae (corresponding to $\dot\theta = 0$). Let us note that the product of the derivatives of Equations (32) and (33), of these two characteristics is -1, indicating that they are orthogonal.

In the one hand ellipses exist when there are solutions $r = r_i = $ constant of Equation (32) for any θ, with $r_i \geq 1 + \sqrt{A}$ or equivalently $\alpha = \alpha_i = $ constant (because $\alpha = r - 1$) with $\alpha_i \geq \sqrt{A}$. Then Equation (32) can be integrated yielding

$$\left(\frac{z}{\alpha_i}\right)^2 + \frac{\rho^2}{\alpha_i^2 - A} = K_1, \tag{34}$$

where K_1 is an integration constant. The comparison of Equation (34), valid for any θ, with Equation (1), implies $K_1 = 1$.

On the other hand, hyperbolae exist when there are solutions of $\cos\theta \equiv \mu = \mu_i = $ constant of Equation (33) for any r, with $\mu_i^2 \leq 1$. These are solutions of the equation $T = 0$,

when $L_z = 0$, with

$$T^2 = \left(\frac{a}{M}\right)^2 (E^2 - 1)\alpha^4 \left[1 - \left(\frac{z}{\alpha}\right)^2\right] \Lambda, \tag{35}$$

where we have defined $\Lambda = \left\{ \mathcal{Q}/[a^2(E^2 - 1)] + (z/\alpha)^2 \right\}$. There are two possible cases, namely $\mu_i^2 = 1$, then $T = 0$ for any $\mathcal{Q}$, or $\mu_i^2 = -\mathcal{Q}/[a^2(E^2 - 1)] = 1 - (\rho_1/\rho_e)^2 \leq 1$, being positively defined only if $\mathcal{Q} \leq 0$, or equivalently, if $\rho_1 \leq \rho_e$. Then, for $\mu_i^2 = 1$, we have $z = r - 1 = \alpha$ and $\rho = 0$ for any r and Equation (33) reduces to $\to \infty$, and the characteristics being along the semi-axis $z \geq \sqrt{A}$. For $\mu_i^2 = -\mathcal{Q}/[a^2(E^2 - 1)]$ we have from Equation (33)

$$\frac{dz}{d\rho} = \frac{z^2 - A\mu_i^2}{z\rho}, \tag{36}$$

which can be integrated leading to

$$\rho = K_2 \left[\left(\frac{z}{\mu_i}\right)^2 - A \right]^{1/2}, \tag{37}$$

where K_2 is an integration constant. Comparing Equation (37), valid for any r, or equivalently for any α, with Equation (1) yields $K_2 + \mu_i^2 = 1$.

Relation (37) represents a family of hyperbolae parametrized by

$$\frac{\rho_1}{\rho_e} = \left(1 - \mu_i^2\right)^{1/2} \tag{38}$$

yielding

$$\frac{1}{A} \left[1 - \left(\frac{\rho_1}{\rho_e}\right)^2\right]^{-1} z^2 - \frac{1}{A} \left(\frac{\rho_1}{\rho_e}\right)^{-2} \rho^2 = 1 \tag{39}$$

If the IC of a geodesic lies inside an ellipse of the type defined by Equation (34), such a geodesic cannot be unbounded and hence cannot go to infinity. So, the allowed IC has to satisfy a triple condition, i.e., i) be inside the ergosphere in order to be possibly issued from a Penrose process; ii) be outside the largest elliptic characteristic, corresponding to the larger value of the roots r_i and iii) be above the higher hyperbolic characteristic,

which corresponds to the highest value of the roots $|\mu_i| \leq 1$. These conditions restrict the permitted domain of IC.

An ellipse, solution of Equation (34), when it exists (i.e. when $r_i \in [1 + \sqrt{A}, \infty[)$, can intersect the ergosphere only if its semi-minor axis $b_i = (\alpha_i^2 - A)^{1/2}$ is smaller than $\rho_e = a/M$, i.e. if $r_i < 2$.

As an example, let us consider again the special case of a double root Y studied previously.

a) The first admissible range is $Y \in [Y_{0b}, 3.869]$ (see Figure 2). These roots, belonging to the domain of physical definition $r \in [1 + \sqrt{A} = 1.86, \infty[$, correspond to the existence of elliptic characteristics. The smallest ellipse has as semi-minor axis $b_i = [(Y - 1)^2 - A]^{1/2} = [(1.88)^2 - 0.75]^{1/2} = (2.78844)^{1/2}$ along ρ, and as semi-major axis $a_i = \sqrt{\alpha_i^2} = Y - 1 = 1.88$ along z, obtained for the smallest value $Y_{0b} \simeq 2.88$, corresponding to $\rho_1/\rho_e \simeq 10.24$. This ellipse contains the ergosphere, the limits of which being $z_{\max} = \sqrt{A} = 0.866$ and $\rho_{\max} = 1/2$. Hence, it is always impossible to have IC simultaneously inside the ergosphere and outside any ellipse. Thus, in this case, it is impossible to have unbound geodesics starting from the ergosphere.

b) For the second admissible range, we found that $Y \in [-0.5, Y_{0a}]$ (see Figure 2). These roots do not belong to the domain of definition of the physical variable r, which means that there is **no** corresponding elliptic characteristic. The only remaining possible limitation depends on the position of the hyperbolic characteristics Equation (39). The hyperbola intersects the z -axis at the point with coordinates $\rho = 0$ and $z_0 = \{A[1 - (\rho_1\rho_e)^2]\}^{1/2}$ and tends asymptotically towards a straight line of equation $\rho \simeq z \tan\theta_1$, with $\sin\theta_1 = \rho_1/\rho_e$. The domain of possible IC is located between the z-axis, the ergosphere and the hyperbola. For example, for $Y = -0.242$, $\rho_1/\rho_e = 0.693$, $\theta_1 = 21^o$, and $z_0 = 0.624(< \sqrt{A} = 0.866)$.

As we have seen, geodesics characterized by $E \to \infty$ may exist. Indeed, trajectories defined by the differential Equation (21) in GMMS10, are well behaved when $E \to \infty$ (but with ρ_1 finite), as can be easily verified by factorizing E in the numerator and the denominator of the second member, leaving a finite quantity when $E \to \infty$. The existence of such trajectories has been verified by the numerical solution of Equation (21) in GMMS10 for high energy values and the corresponding values of ρ_1 as described in Section 3. Of course, the value of the energy will be always finite and fixed by the particular Penrose process which takes place at the origin of these particular geodesics inside the ergosphere. The main point resulting from the present investigation is that if very energetic particles are produced as a consequence of such a process, there are unbound geodesics that will be followed by those particles, which will permit their ejection in a collimated way along the spin axis of the black hole.

In Figure 3 is plotted the geodesic which tends asymptotically towards the corresponding value $\rho = \rho_1 = 0.347$, for which the test particle has a very high (theoretically "infinite", but for present calculations, we took value $E = 10^6$ and $\rho_1/\rho_e = 0.693$). This plot corresponds to the IC $\rho_i = 2.8 \times 10^{-6}$ and $z_i = 0.8521$, which correspond to a point just inside the ergosphere at its top near the z-axis, i.e., near the event horizon. For the other limit $(Y = -0.5)$, $\rho_1 = 0$, $E = \sqrt{3}$, $\theta_1 = 0$ and $z_0 = \sqrt{A} = 0.866$.

In order to illustrate the considered geometry, we have plotted in Figure 4 the relevant curves and surfaces like the ergosphere, the critical hyperbola, a possible unbound geodesic and its corresponding asymptote. Curves in black and with subscript a correspond to the case $a/M = 0.5$ considered above, while curves in red and with subscript b correspond to the extreme case $a/M = 1$. The geodesic for the case $a/M = 1$ was calculated for the following values of the constants: $E = 10^6$ and $\rho_1 = 0.8284$ (see end of Section 3) and for
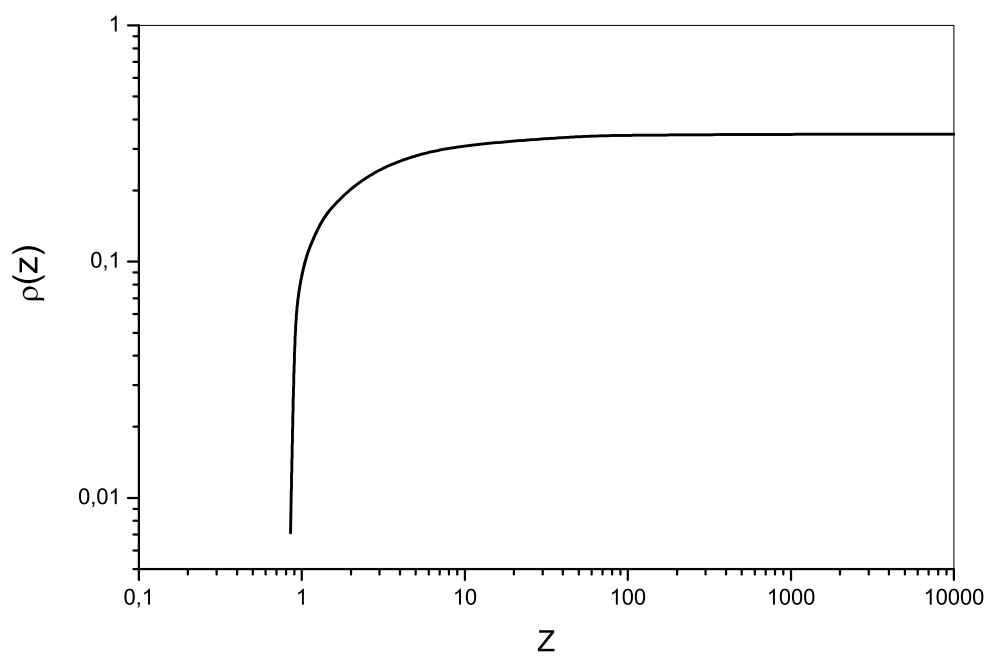
Fig. 3.— Plot of the geodesic $\rho(z)$ for a Kerr BH characterized by $M = 1$ and a spin parameter $a/M = 0.5$. The constants of motion and initial conditions are those given in the text.

the following IC, $\rho_i = 0.1$ and $z_i = 0.1675$. Notice that in the extreme case, the critical hyperbola, which delimitates with the ergosphere and the z-axis the region where unbound geodesics emerge, degenerates into a straight line starting from the origin and having a slope $\Delta z/\Delta \rho \simeq 0.676$. Moreover, the high energy beam of geodesics has a width, measured by the distance between the z-axis and the asymptote, which is about a factor of two larger than that obtained for the case $a/M = 0.5$.

Let us return to the case $a/M = 0.5$. By modifying a little bit the preceding IC, we find other geodesics similar to the latter ones but diverging or, in other words, deviating slightly from its asymptote ρ_1. For instance, taking as IC $\rho_i = 2.8 \times 10^{-6}$ and $z_i = 0.852086175$ we obtain a geodesic that diverges almost rectilinearly from the turning point at $\rho \simeq 0.3466$ and $z \simeq 50 \times 10^3$ attaining at $z = 10^{10}$ (or 1 Mpc) the abscissa $\rho \simeq 350$ (or 3×10^{-2} pc), which corresponds to a slight slope $\Delta \rho/\Delta z = 3.5 \times 10^{-8}$. This geodesic conserves its highly collimated character. If this geodesic is followed by an electron, its kinetic energy converges to the total energy E, attaining at $z = 10^{10}$ (or 1 Mpc from the BH) a Lorentz factor $\Gamma = 5 \times 10^4$, which corresponds to an energy 25 GeV. This same electron at $z = 1.4 \times 10^9$ (or 140 kpc), where $\rho \simeq 50$ (or 5×10^{-3} pc), attains a Lorentz factor $\Gamma \simeq 1.9 \times 10^4$ or an energy of the order 9.4 GeV.

The local Lorentz factor along a given geodesic is defined by its usual expression $\Gamma = (1 - v^2/c^2)^{-1/2}$, where $v^2 = v_z^2 + v_\rho^2$, $v_z = \dot{z}/\dot{t}$ and $v_\rho = \dot{\rho}/\dot{t}$. The overdot means the derivative with respect to the proper time τ. Gravitational effects are included self-consistently in the expressions defining the Kerr geodesics. In this way, Γ can be expressed as a function of the coordinates ρ and z. For the case previously considered (geodesic shown in Figure 3), the variation of the Lorentz factor along the geodesic can be expressed as a function of the coordinate z alone. The result is shown in Figure 5. Notice that in the beginning the energy is essentially under the form of potential energy ($\Gamma \simeq 1$),
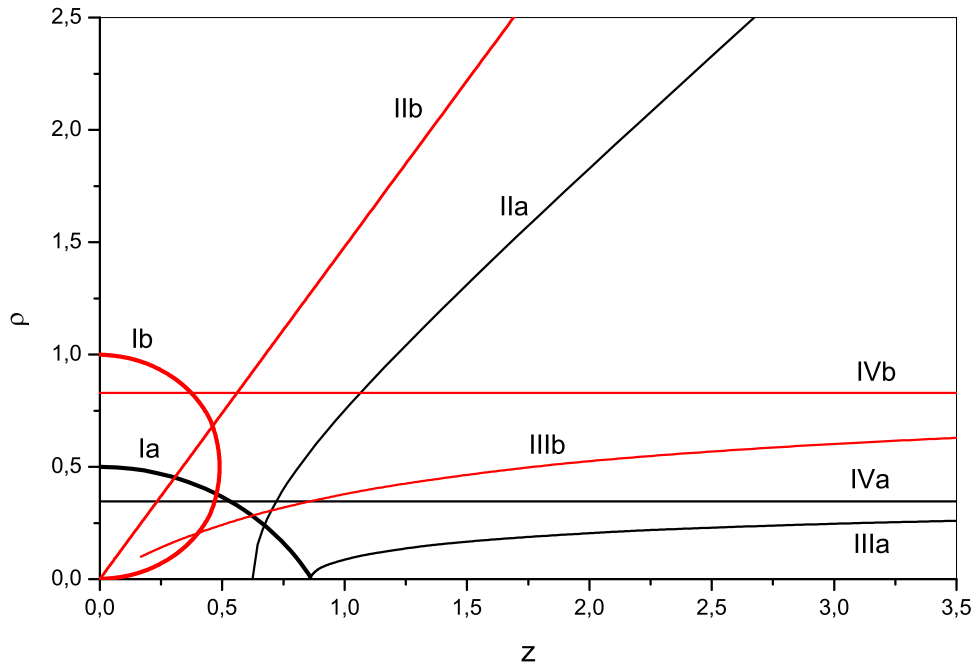
Fig. 4.— The ergosphere (labels Ia and Ib), the critical hyperbola (labels IIa and IIb), an example of a unbound geodesics (labels IIIa and IIIb) and the respective asymptotes (labels IVa and IVb) are shown for black holes having a spin parameter $a/M = 0.5$ (black curves) or $a/M = 1$ (red curves).

while far from the ergosphere, the energy is essentially kinetic.

6. Conclusions

Taking the roots of the characteristic equation for unbound 2D-geodesics with $L_z = 0$ as free parameters, we have shown that the two remaining constants of motion, E and $\mathcal{Q}$, of a test particle following geodesics that asymptotically tend to a parallel line to the z-axis, can be expressed as a function of the aforementioned parameters. In the particular case of a double root and assuming a spin parameter to be equal to $a = M/2$, restricted domains of asymptotes corresponding to high particle energies are found. This means that the Kerr metric can generate powerful collimated jets of high energy particles in some well defined regions inside the ergosphere. Indeed, for this special case, only two possible ranges of ρ_1 are possible, namely $\rho_1 \in [0.3382, 0.3466]$ and $\rho_1 \in [5.12, 5.34]$ for $E \in \left[\sqrt{6}, \infty\right[$ and $E \in \left]\infty, \sqrt{3}\right]$ respectively (see Figure 2).

It is worth mentioning that the present results are a strict consequence of the structure of the Kerr metric. The main approximation is the assumption of the existence of a double real root Y for the characteristic equation. Although we have considered in some more detail the case of a moderately spinning black hole ($a/M = 0.5$), the results are qualitatively the same for the case of a extreme Kerr black hole. We hope that by relaxing the double root hypothesis, maybe it would be possible to obtain thicker beams of energetic particles. An investigation is currently in progress and preliminary results are encouraging.

Two positions of the asymptote corresponding to an "infinite" energy in our model are $\rho_1 \simeq 5M$ and $\rho_1 \simeq 0.3466M$. The latter is the only case compatible with the limitations imposed by the characteristics of the system of geodesic equations, according to our discussion in Section 5. The consequence of these mathematical constraints is that the
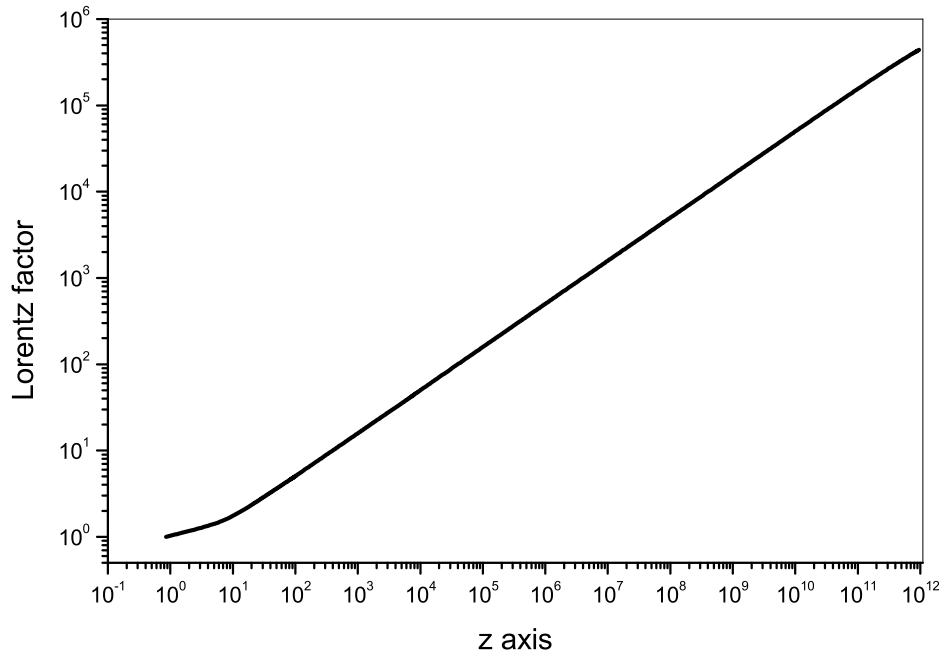
Fig. 5.— Lorentz factor as a function of the coordinate z for the geodesic shown in Figure 3.

resulting jet is very narrow. However, there is some observational evidence for the presence of radial flows in some jets (Giroletti et al. 2004) and, as already mentioned, they may have a two-component flow, i.e., a relativistic powerful inner jet and a slower, less powerful outer flow (De Villiers et al. 2005; Xie et al. 2012). The present model could be related to the inner flow which carries most of the power, being constituted mainly by relativistic particles.

Our results can also easily be extended to particles other than electrons, for example protons or heavy nuclei. This does not modify the "geometry" that we obtained, i.e., the positions ρ_1 of the jets, but their energy only. For a proton ($c^2\sqrt{\delta_1} \simeq 1$ GeV) the maximal energy we can here numerically calculate (which is theoretically as large as wanted) is about $E \simeq 5.6 \times 10^{25}$ eV $= 5.6 \times 10^7$ EeV, which largely includes the highest energies of the current observed UHECR (Dermer et al. 2009; Hoover et al. 2010). Thus, our model could be relevant to explain not only a collimated flux of relativistic particles but also the production of these very energetic particles that could be related to UHECR. A detailed analysis of the Penrose process and of its efficiency is beyond the aim of this paper. Nevertheless, we would expect that the rate of emerging particles would be proportional to the accretion rate and to the ratio between the volume of the region in the ergosphere where unbound geodesics exist and the total volume of the ergosphere. A simple example of a Penrose event could be the ionization of the inner shells of an iron atom inside the ergosphere, with the nucleus being captured by the BH and the electron being ejected with a high energy. The accreted gas near the ergosphere has temperatures around 10^6 K (Montesinos & de Freitas Pacheco 2011), high enough to ionize the K-L shells of iron, providing a theoretical basis for such a possibility.

Recent results of the Pierre Auger Observatory (Roulet 2009) suggest a correlation between UHECR above 57 EeV and nearby (< 70 Mpc) AGNs. Since in the present

model the collimation of the relativistic particles occurs along the spin axis, it would be interesting to investigate if the associated AGNs are of type I or II, since in the context of the "unified model" these classes differ only by the inclination of the jet axis with respect to the line-of-sight.

Let us recall briefly that since our model does not require magnetic fields, it can be applied to neutral particles as, for instance, neutrinos. If they have a mass of $\sqrt{\delta_1} = 0.33$ eV (Steidl 2009), according to our previous estimate, they could attain energies of the order of $E \simeq 2 \times 10^{-2}$ EeV.

Finally, different authors have recently discussed the possibility to produce high energy particles by collisions near a rotating BH (Grib & Pavlov 2011), raising the interest of having further investigations on the Penrose process (see also Bañados at al 2011). The present investigation can be seen as an additional contribution to this debate.

REFERENCES

Bañados M., Hassanain B., Silk J. and West M., 2011, Phys.Rev. D 83, 023004

Blandford R.D. and Levinson A., 1995, ApJ 441, 79

Camenzind M., 2005, Mem.Soc.Astron.It. 76, 98

Chandrasekhar S., 1983, *The Mathematical Theory of Black Holes*, Oxford University Press, Oxford

Dermer C.D., Razzaque S., Finke J.D. Atoyan A., 2009, New J.Phys. 11, 065016

De Villiers J.P., Hawley J.F, Krolik H.H. and Hirose S., 2005, ApJ 620, 878

Frail D.A., Kulkarni S.R., Sarl R. et al., 2001, ApJ 562, L58

Gariel J., MacCallum M.A.H., Marcilhacy G. and Santos N.O., 2010, A& A 515, A15 - (GMMS10)

Giroletti M., Giovannini G., Feretti L. et al., 2004, ApJ 600, 127

Grib A.A. and Pavlov Y.V., 2011, Grav.& Cosmol. 17, 42

Guo F. and Mathews W.G., 2011, ApJ 728, 121

Hoover S., Nam J., Gorham P.W. et al., 2010, arXiv:1005.0035v2.

Keppens R., Meliani Z., van der Holst B. and F. Casse F., 2008, A& A 486, 663

Marscher A.D., in Multiband Approach to AGN, eds. A.P. Lobanov and T. Venturi, 2005, Mem.Soc.Astron.It. 76, 168

Meier D.L., Koide S. and Uchida Y., 2000, Science 291, 84

Meliani Z. and Keppens R., 2009, ApJ 705, 1594

Mészáros P., Rees M.J. and Wijers R.A.M., 1999, New Astron. 4, 3

Montesinos M. and de Freitas Pacheco J.A., 2011, A&A 526, A146

Pontriaguine L., 1975, *Equations Differentielles Ordinaires*, Editions Mir, Moscow

Rossi E., Lazzati D. and Rees M.J., 2002, MNRAS 332, 945

Roulet E., 2009, Nucl. Phys B 190, 169

Steidl M., 2009, arXiv:0906.0454v1.

Vlahakis N. and Konigl A., 2004, ApJ 605, 656

Xie W., Lei W.-H., Zou Y.-C., Wang D.-X., Wu Q. and Wang J.-Z., 2012, arXiv: 1202.5024v1.